International Journal of Innovative Technology and Interdisciplinary Sciences
https://journals.tultech.eu/index.php/ijitis
ISSN: 2613-7305
Volume 9, Issue 1
DOI: https://doi.org/10.15157/IJITIS.2026.9.1.311-335
Received: 04.09.2025; Revised: 22.01.2026; Accepted: 02.02.2026

Research Article

Enhancing Voltage Profile and Power Factor in SLD Distribution Networks via Radial and Cyclic Configurations with Solar Integration

Jyoti Gupta*, Gopalasamy Selvakumar

Department of Electrical and Electronics Engineering, Aarupadai Veedu Institute of Technology, Vinayaka Mission's Research Foundation (DU), India

***er.jyoti2108@gmail.com**

Abstract

This study explores the enhancement of voltage stability and power factor in single-line diagram (SLD) networks by integrating solar energy within radial and cyclic systems. As electricity demand rises, effective demand-side management (DSM) becomes essential for optimizing energy consumption and improving grid reliability. The research highlights the challenges posed by voltage fluctuations and power factor imbalances when incorporating solar energy into existing power distribution networks. Utilizing load flow analysis via Electrical Transient Analyzer Program (ETAP), the study evaluates power losses, voltage profiles, and power factor variations across three scenarios: (1) Base Radial Network, (2) Optimized Radial System with photovoltaic (PV) and Capacitors, and (3) Cyclic System with PV and Capacitors, aiming to implement corrective measures for improved power quality. The methodology involves a comprehensive analysis of a 500kW grid-connected solar PV system, including calculations for energy generation, inverter selection, and land area requirements. The findings indicate significant improvements in voltage regulation (from 0.89 p.u. to 0.96 p.u.) and power factor (from 0.85 lagging to 0.98 lagging) through strategic modifications to distribution transformer ratings and the addition of capacitor banks. Crucially, a sensitivity analysis, varying solar irradiance by ±20%, confirms the robustness of the proposed Cyclic System against environmental fluctuations, yielding a system Voltage Deviation Index (VDI) improvement of 48% under the worst-case cloudy scenario. Simulation results demonstrate that the integration of solar energy not only mitigates overloading issues but also enhances overall system performance, reducing power losses and operational costs. The study concludes that the proposed DSM framework, leveraging real-time solar energy forecasting and adaptive techniques, offers a scalable solution for modern electrical networks, ensuring sustainable and reliable power distribution.

Keywords: Demand Side Management; Single-Line Diagram; Load Flow Analysis; Voltage Balance; Power Factor Balance; ETAP Simulation.

INTRODUCTION

With the increased demand for electricity to integrate renewable energy resources, efficient power management has become crucial to ensure a stable power supply with

reliability in the distribution side. Demand-side management (DSM) plays a major role in optimizing energy consumption by adjusting the power demand pattern of the consumers to emphasise grid efficiency [1]. In the present scenario, hybrid grid facilities have to be integrated into the existing distribution system. The adoption of sustainable energy is important to the generation system, which can be initiated with wind and solar energy. Solar and wind power are abundant source of energy. The working of a solar panel increases the power generation on the grid. On the other hand, wind energy also contributes the wind energy for the power generation, with the help of a turbine, which works on the Wind Energy Conversion System (WECS) [2, 3]. In this system turbine works on the principle of Direct Torque Control (DTC), which uses an induction motor to directly control torque and flux, offering a fast dynamic response and robust operation under voltage dips. This method of DTC is enhancing the robustness of the turbine. This role can be adopted for generation and power distribution purposes for the industrial sectors rather than the residential [4]. In the residential sector, solar energy generation will be suitable for power generation to support the grid or substation for distribution. It will help to supply the power for the peak demand of consumers. For these systems, DSM strategies help to reduce peak load, enhance system durability to minimize operational costs, making power distribution more sustainable and improving its efficacy. However, one of the major challenges in DSM is maintaining optimal voltage levels as well as power factor for overall power quality improvement [5]. A regulated voltage drop with a low power factor will lead to energy losses in equipment with inefficiencies as well as increased operational costs for utilities [6].

With the growing emphasis on renewable energy, solar power is an emerging and viable solution to fulfil the increased energy demand with carbon emission reduction [7]. The integration of solar energy into power distribution networks, especially in radial and cyclic single-line diagram (SLD) systems, has presented several technical challenges, which help to improve voltage fluctuations with power factor imbalances. To ensure the efficacy of the energy distribution system, load flow analysis is essential to evaluating the power losses, voltage profiles, and power factor variations in the system [8, 9].

Electrical Transient Analyzer Program (ETAP) has been frequently used for power system analysis, which provides accurate simulation to evaluate network performance, optimize load flow as well as improve power quality [10]. ETAP simulation enables engineers to analyse different DSM strategies to assess voltage drop with the power factor variations for implementing corrective measures to enhance the grid reliability. Despite advancements in ETAP-based optimization techniques, there remains a significant research gap in addressing the dynamic impact of solar integration on voltage drop and power factor regulation for the radial and cyclic SLD configurations [11]. In the existing system, studies often lack real-time analysis of the practical implementation of DSM techniques tailored for solar-powered networks. Because of these barriers, real-time simulation has been started with the software. To improve the research accuracy level with the efficacy [12].

LITERATURE STUDY

The focus is on new developments in demand-side energy management systems (DSEMS) that improve energy efficiency with durability. It covers many methods with different technologies created to reduce consumer expenses and increase energy efficiency. The article focuses on how real-time data analytics and smart meters will help emphasise energy management [1, 13]. The framework of smart grids, demand-side energy management, is deeply examined in this overview. Major barriers include technological integration, consumer engagement, and regulatory concerns. The authors suggest ways to emphasise the DSEMS in the future scope, such as integrating sophisticated communication technology with sustainable energy resources [5, 14]. To optimise the residential customers' energy consumption, a probabilistic load shifting technique has been used. Unbalancing the energy supply and the demand has been considered by the method, which offers a more reliable, sustainable, adaptable and flexible load management approach. Simulation findings show that the suggested strategy is a successful process for lowering the peak load to improve energy efficacy [6, 15]. An approach to shift the load in microgrid-based swarm intelligence, which is represented in this research work with an emphasis on the financial and ecological advantages. To optimise load distribution as well as reduce operating costs, the method makes use of algorithms that are designed after the natural event. Significant gains in the microgrid performance, such as improved reliability, which lowers emissions, are shown by the results [7, 16]. A multi-objective hybrid optimisation method for demand-side management in smart buildings has been considered. Simulations are used to show the effectiveness of the technique to strike a balance between cost savings, occupant comfort, and energy efficiency. According to the result, the suggested approach can greatly emphasise energy management in smart buildings [8, 17].

It has suggested a brand-new approach to developing daily load profiles which accounts for fluctuations in the power supply within the demand for energy from renewable sources. According to the research, adding RES can result in load profiles that are steadier with more predictable, which would eventually increase the microgrid's operational efficacy. Case studies show that implementing optimised load profiles significantly lowers operating costs and improves energy reliability [9, 18]. To optimise the utilisation of hybrid photovoltaic (PV) and wind energy resources within a demand-side management framework by designing an autonomous fuzzy controller. The recommended controller emphasises energy systems' reliability by efficiently balancing supply with consumer demand. In comparison to the simulation result of conventional approaches of the energy management performance has been enhanced [10, 19]. Using K-mean clustering with integer programming, the recommendation of a consumer-driven demand-side management approach to maximise energy use in an independent renewable energy grid. The method makes it possible to have a better supply of energy and better meet the demand of consumers, which emphasises the grid's efficacy as well as stability. For consumer satisfaction, energy management has to be significantly improved [13, 20]. The optimal operation of responsive loads to emphasise the energy efficiency is the main topic of this research, which discusses energy rescheduling in multi-energy systems. By efficiently coordinating several energy resources as well as loads, these suggested scheduling algorithms lower operating costs and enhance the system performance of the system. The article emphasises how crucial to incorporate responsive loads into energy management plans [14]. Optimising energy output with efficiency is the main goal of the authors' energy management plan for a 50 kW Proton Exchange Membrane Fuel Cell (PEMFC) hybrid system. The plan uses real-time monitoring as well as a control system to improve system performance in different load scenarios. According to simulation results, energy utilization and system reliability are greatly increased by the suggested management approach [15, 21-22].

The increasing integration of intermittent distributed generation (DG), particularly solar photovoltaic (PV), has necessitated a strategic shift towards advanced distribution network management to maintain stability and power quality. The recent literature strongly advocates for structural modifications and optimization to address these challenges [23-25]. Several studies emphasize the benefit of network reconfiguration and cyclic systems over traditional radial feeders, showing that they significantly improve reliability metrics like the System Average Interruption Frequency Index (SAIFI) [26, 27]. Complementing this, other works focus on mitigating the voltage and power factor issues inherent to PV integration: optimization techniques are now widely utilized for Voltage Deviation Index (VDI) minimization [28] and for the optimal placement of corrective devices, such as shunt capacitors, to ensure robust power factor correction under variable irradiance conditions [29]. The most advanced solutions combine these strategies; for instance, multi-objective frameworks simultaneously optimize network reconfiguration and the placement of components like D-STATCOMs [30] or battery energy storage systems (BESS) [31] to ensure both quality and reliability. Furthermore, the role of Demand Side Management (DSM) has been crucial in complementing PV integration to enhance voltage profiles and reduce power losses [32]. Crucially, the practical relevance of these findings is supported by research detailing the sensitivity of voltage stability to irradiance and temperature [33], and by validated load flow modelling using tools like ETAP on real-world utility networks [34] and standard test systems like [35].

The paper's scalability as well as effectiveness for the practical examples of successful DSEM implementations may be limited due to a lack of empirical data, in-depth case studies, cultural behavioural factors and the complexity of swarm intelligence algorithms. Additionally, the research doesn’t consider renewable energy sources' variability in microgrid operation [36-38]. The research observations on fuzzy controllers are not applicable in real-world scenarios due to reliance on simulation results. Lack of detail on occupant comfort-energy savings trade-offs and insufficient consideration of renewable energy sources' versatility. The focus on commercial as well as industrial sectors will limit applicability for residential microgrid systems. Thus, the fuzzy controller's effectiveness will vary under different environmental conditions with the energy demand scenario. The research limitations include not considering external factors, long-term operational challenges, and specific power output.

To bridge this gap, this research focuses on creating an advanced DSM framework by utilizing ETAP simulation to optimize voltage and power factor balancing in solar-integrated radial and cyclic SLD systems. The proposed methodology aims to implement intelligent load flow optimization, ensuring grid reliability with efficient power distribution. This research seeks to provide a practical and scalable solution for emphasising power quality in modern electrical networks by incorporating solar energy forecasting in real-time load adjustments with adaptive DSM techniques. In this article, the author's strategies can be implemented for the voltage improvement, power factor improvement and to reduce the branch power losses at the feeder. It can be used in any type of feeder to improve these parameters with sustainable energy in the distribution without compromising the required parameter standards of voltage and power factor.

PROBLEM FORMULATION

The core of the analysis relies on load flow simulations executed within the ETAP platform, utilizing a modified IEEE 33-Bus Distribution Test System adapted to represent a 11 kV Indian distribution feeder (TNPDCL topology).

Mathematical Model for Network Analysis

The assessment of the distribution network performance is quantified using the following fundamental equations derived from the load flow analysis.

Power Flow and Voltage Drop

For any branch connecting bus i to bus j, the voltage drops (ΔV_{ij}) and power loss ($P_{Loss,ij}$) are calculated as equation (1):

$$\Delta V_{ij} = Z_{ij} \frac{P_j + jQ_j}{V_i^*} \tag{1}$$

where Z_{ij} is the impedance of the branch, P_j and Q_j are the real and reactive power demanded at bus j, and V_i is the voltage at bus i.

Real Power Loss in the Line ($i - j$)

The total real power loss in the system ($P_{TotalLoss}$) is the sum of losses across all branches:

$$P_{Loss,ij} = R_{ij} \frac{\left(P_j^2 + Q_j^2\right)}{\left|V_j\right|^2} \tag{2}$$

$$P_{TotalLoss} = \sum_{i=1}^{N_{br}} P_{Loss,ij} \tag{3}$$

Voltage Deviation Index (VDI)

VDI is introduced as a metric to quantitatively assess the voltage stability improvement across the entire network.

$$VDI = \frac{1}{N} \sum_{k=1}^{N} \left(\frac{V_{nominal} - V_k}{V_{nominal}} \right)^2 \tag{4}$$

Lower VDI indicates a flatter and more stable voltage profile.

PV Array Equation and Calculation for a 500 kW Grid-Connected Solar System

A grid-connected solar PV system does not require a battery storage system, as excess energy is transferred into the grid, and power is drained from the grid when solar production is at a minimum.

Step -I: PV Array Equation

The power generated by a PV array depends on the number of panels and their capacity, see equation (5):

$$P_{array} = N_P * P_{Panel} \tag{5}$$

Where,

P_{array} - Total power of the array (W or kW)

N_P - Number of solar panels

P_{Panel} - Power rating of one solar panel (W)

Solar radiation and system efficiency decide the overall amount of energy produced each day.

$$E_{daily} = P_{array} * H_{sun} * \eta \quad (6)$$

Where,

E_{daily} - Daily energy output (Wh or KWh)

H_{sun} - Average peak Sun hour/day

η - System efficiency (80-90%)

Step – II: Calculate the number of solar panels

Let's assume 240W (0.24kW) solar panels.

$$Number\ of\ panels = \frac{Total\ capacity\ (kW)}{Panel\ capacity\ (kW)} \quad (7)$$

$$N_P = \frac{500}{0.24} = 2084\ panels \quad (8)$$

Hence, 2084 panels of 240W each.

Step – III: Energy Generation estimate

If the system receives 5 peak sun hours/day, from equation (6)

$$E_{daily} = 240 * 5 = 1200\ kWh/day$$

$$E_{annual} = 1200 * 365 = 4{,}38{,}000\ kWh/year$$

This energy is directly fed to the grid.

Step – IV: Inverter Selection

The nature of the electrical system connection to the grid, an inverter is necessary to transform solar panels' DC power into AC. The inverter and the entire system should have equivalent capacity.

$$P_{inverter} = P_{array} = 500\ KW$$

If using 100 kW inverters, the number required:

$$N_i = \frac{500}{100} = 5\ inverters$$

Where, N_i = Number of Inverters

Step – V: String Configuration (Voltage and Current)

Each 240W solar panel typically has:

Voltage (Vmp) = 30.65V

Current (Imp) = 7.82A

Panels have to be set up in parallel and series strings according to the input voltage for the inverter.

Series Connection (Voltage Matching):

If the inverter operates at 1000V DC, the number of panels in series

$$N_{10} = \frac{1000}{30.65} = 33\ panels\ per\ string$$

Parallel Connection (Current Distribution):

Total number of strings required:

$$N_p = \frac{2084}{33} = 64\ parallel\ strings$$

Total current:

$$I_{array} = 64 * 7.82 = 500.48\ A$$

Step – V: Land Area Requirement

Each 240W panel has an approximate area of 1.6 m^2.

Total panel area = $2084 * 1.6 = 3334.4\ m^2$

Considering space for maintenance and shading, the total land required is as follows:

$$3334.4 * 0.8 = 2667.52\ m^2\ (0.7\ acre)$$

ETAP Simulation Setup for Reproducibility

The detailed ETAP simulation parameter and its values are given in Table 1 to ensures the full reproducibility of the given work, see Table 1.

Table 1. ETAP simulation parameters

Parameter	Value	Description
Simulation Software	ETAP 20.0.0	Electrical Transient Analyzer Program
Load Flow Method	Newton-Raphson	Chosen for its high accuracy and convergence speed.
Convergence Tolerance	0.001 p.u.	The maximum magnitude of the power mismatch at any bus.
Maximum Iterations	100	Safeguard limit for non-convergent cases.
System Base Values	11 kV, 10 MVA	Standard base for the distribution network.
Solar PV Integration	500 kW at Bus 6 (P-V Bus)	Modelled as a P-V generator, injecting fixed real power and regulating voltage.
Load Modelling	Constant Power (PQ Bus)	All distribution loads are modelled as constant P and Q loads.
Capacitor Sizing	450 kVAR (distributed)	Optimized based on the maximum reactive power demand observed in the Base Case.

The work aims to provide a sustainable and uninterrupted power supply to the consumer with adaptive demand-side management techniques. For sustainability, solar

energy will be added to the grid to fulfil the power demand without any compromise in the voltage rating or power factor. This will support the grid during peak demand times and also make the supply sustainable. For comparative analysis, the load flow analysis has been performed for three distinct scenarios:

Base Radial System: The original modified IEEE 33-bus network configuration. Radial System with PV and Capacitors: Integration of the 500kW PV plant and optimized shunt capacitors (450 kVAR) into the base radial structure. Proposed Cyclic System with PV and Capacitors: The network is reconfigured into a cyclic (looped) topology to enhance reliability and redundancy, maintaining the integrated PV and capacitors.

DATA OBSERVATION

Figure 1 depict the Simulation diagram of load flow analysis of existing system SLD and the network SLD system of dt 13

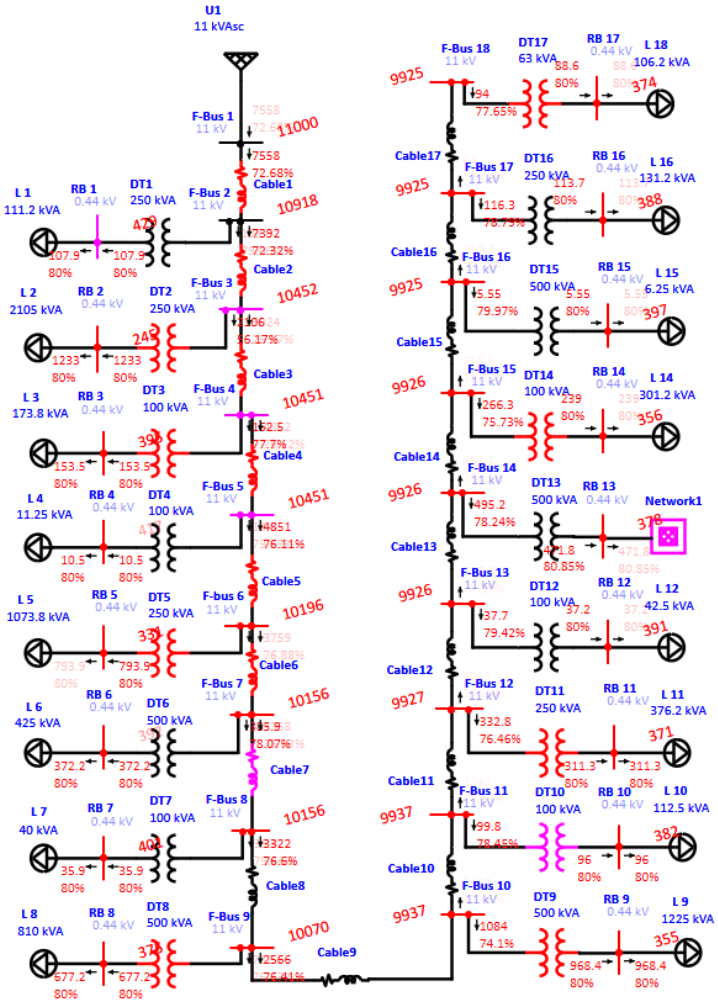

(a)

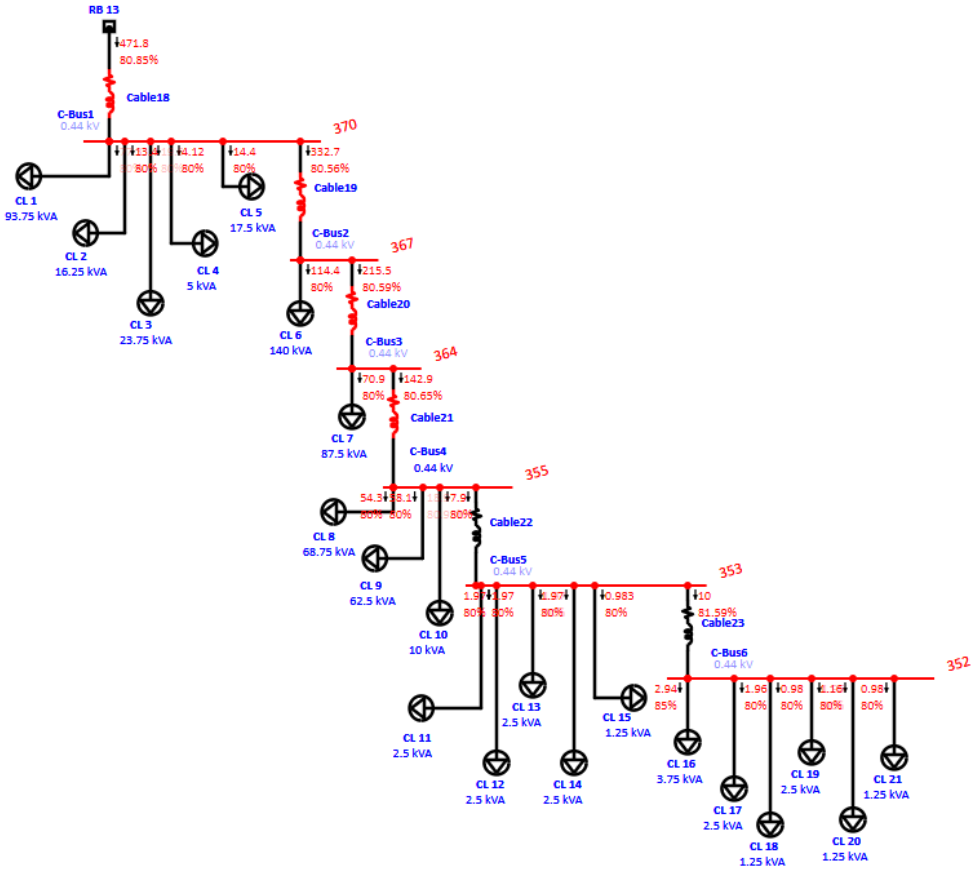

(b)

Figure 1. (a) Simulation diagram of Load Flow Analysis of Existing System SLD, (b) Simulation diagram of Network SLD system of DT 13

The above SLD represents the existing system SLD for the feeder bus bar system. This SLD has been drawn and simulated in the ETAP simulation software for the load flow analysis report, which helps to rectify the voltage drop and power factor imbalance in the feeder. With the help of load flow analysis, power losses can be reduced in the feeder. Here, it can be seen in this given feeder SLD Cable 1, 2, 3, 4, 5 & 6 and DT-2, 3, 5, 8, 9, 10, 11, 14 & 17 are overloaded condition. After completing the load flow analysis using the Newton-Raphson Method, the feeder problem has been identified, as shown in Figure 1(a), as per Figure 1(b). The buses are under voltage conditions. This SLD is a network SLD, which is an expansion of DT-13 distributed load data. Hence, this under-voltage, overloading of DTs and cables has to be reduced with the help of the simulation method.

Table 2 represents the F-bus, RB and C-bus voltage drop data with distributed load data in KW. Majorly voltage has occurred because of the overload on the bus bar system. This overloading occurs due to the excessive consumption of power from the sanctioned distributed load

Table 2. Voltage drop data of the feeder buses

Bus ID	Nominal kV	Voltage	kW Loading
C-Bus1	0.44	0.37	371
C-Bus2	0.44	0.367	265.1
C-Bus3	0.44	0.364	172
C-Bus4	0.44	0.355	111.6
C-Bus5	0.44	0.353	15.23
C-Bus6	0.44	0.352	8.13
F-Bus 1	11	11	5492.6
F-Bus 2	11	10.918	5432.7
F-Bus 3	11	10.452	5009.9
F-Bus 4	11	10.451	3826.9
F-Bus 5	11	10.451	3700.5
F-bus 6	11	10.196	3569.3
F-Bus 7	11	10.156	2874.7
F-Bus 8	11	10.156	2573.3
F-Bus 9	11	10.07	2515.4
F-Bus 10	11	9.937	1926
F-Bus 11	11	9.937	1122.4
F-Bus 12	11	9.927	1042.7
F-Bus 13	11	9.926	788.2
F-Bus 14	11	9.926	758.2
F-Bus 15	11	9.926	370.7
F-Bus 16	11	9.925	169.1
F-Bus 17	11	9.925	164.6
F-Bus 18	11	9.925	72.97
RB 1	0.44	0.429	86.35
RB 2	0.44	0.245	986.2
RB 3	0.44	0.395	122.8
RB 4	0.44	0.417	8.44
RB 5	0.44	0.331	635.1
RB 6	0.44	0.392	297.8
RB 7	0.44	0.401	28.74
RB 8	0.44	0.375	541.7
RB 9	0.44	0.355	774.7
RB 10	0.44	0.382	76.8
RB 11	0.44	0.371	249
RB 12	0.44	0.391	29.74
RB 13	0.44	0.378	381.4
RB 14	0.44	0.356	191.2
RB 15	0.44	0.397	4.44
RB 16	0.44	0.388	91
RB 17	0.44	0.374	70.91

Table 3 depict the load flow analysis report generated through ETAP simulation.

Table 3. Load flow analysis report generated through ETAP simulation

LOAD FLOW REPORT

Bus		**Voltage**		**Generation**		**Load**		**Load Flow**					**XFMR**
ID	kV	% Mag.	Ang.	MW	Mvar	MW	Mvar	ID	MW	Mvar	Amp	%PF	%Tap
C-Bus1	0.440	84.070	0.7	0.000	0.000	0.103	0.077	RB 13	-0.371	-0.274	720.2	80.4	
								C-Bus2	0.268	0.197	519.2	80.6	
C-Bus2	0.440	83.351	0.8	0.000	0.000	0.091	0.069	C-Bus1	-0.265	-0.196	519.2	80.4	
								C-Bus3	0.174	0.128	339.2	80.6	
C-Bus3	0.440	82.705	1.0	0.000	0.000	0.057	0.043	C-Bus2	-0.172	-0.127	339.2	80.4	
								C-Bus4	0.115	0.084	226.7	80.6	
C-Bus4	0.440	80.613	1.5	0.000	0.000	0.096	0.072	C-Bus3	-0.112	-0.083	226.7	80.1	
								C-Bus5	0.015	0.011	30.8	80.9	
C-Bus5	0.440	80.226	1.6	0.000	0.000	0.007	0.005	C-Bus4	-0.015	-0.011	30.8	80.9	
								C-Bus6	0.008	0.006	16.4	81.6	
C-Bus6	0.440	79.999	1.6	0.000	0.000	0.008	0.006	C-Bus5	-0.008	-0.006	16.4	81.5	
F-Bus 1	11.000	100.000	0.0	5.493	5.191	0.000	0.000	F-Bus 2	5.493	5.191	396.7	72.7	
F-Bus 2	11.000	99.251	0.2	0.000	0.000	0.000	0.000	F-Bus 1	-5.433	-5.172	396.7	72.4	
								F-Bus 3	5.346	5.105	390.9	72.3	
								RB 1	0.087	0.067	5.8	79.1	
F-Bus 3	11.000	95.016	1.5	0.000	0.000	0.000	0.000	F-Bus 2	-5.010	-4.998	390.9	70.8	
								F-Bus 4	3.827	3.255	277.5	76.2	
								RB 2	1.183	1.742	116.3	56.2	
F-Bus 4	11.000	95.013	1.5	0.000	0.000	0.000	0.000	F-Bus 3	-3.827	-3.255	277.5	76.2	
								F-Bus 5	3.701	3.153	268.6	76.1	
								RB 3	0.126	0.102	9.0	77.7	
F-Bus 5	11.000	95.011	1.5	0.000	0.000	0.000	0.000	F-Bus 4	-3.701	-3.153	268.6	76.1	
								F-bus 6	3.692	3.147	268.0	76.1	
								RB 4	0.008	0.006	0.6	79.9	
F-bus 6	11.000	92.689	2.1	0.000	0.000	0.000	0.000	F-Bus 5	-3.569	-3.107	268.0	75.4	
								F-Bus 7	2.890	2.404	212.8	76.9	
								RB 5	0.680	0.704	55.4	69.5	
F-Bus 7	11.000	92.332	2.2	0.000	0.000	0.000	0.000	F-bus 6	-2.875	-2.399	212.8	76.8	
								F-Bus 8	2.573	2.158	190.9	76.6	
								RB 6	0.301	0.241	21.9	78.1	
F-Bus 8	11.000	92.330	2.2	0.000	0.000	0.000	0.000	F-Bus 7	-2.573	-2.158	190.9	76.6	
								F-Bus 9	2.544	2.136	188.8	76.6	
								RB 7	0.029	0.022	2.1	79.5	
F-Bus 9	11.000	91.547	2.4	0.000	0.000	0.000	0.000	F-Bus 8	-2.515	-2.126	188.8	76.4	
								F-Bus 10	1.961	1.656	147.1	76.4	
								RB 8	0.554	0.471	41.7	76.2	
F-Bus 10	11.000	90.336	2.7	0.000	0.000	0.000	0.000	F-Bus 9	-1.926	-1.644	147.1	76.1	

								F-Bus 11	1.122	0.916	84.2	77.5
								RB 9	0.804	0.728	63.0	74.1
F-Bus 11	11.000	90.336	2.7	0.000	0.000	0.000	0.000	F-Bus 10	-1.122	-0.916	84.2	77.5
								F-Bus 12	1.044	0.854	78.4	77.4
								RB 10	0.078	0.062	5.8	78.4
F-Bus 12	11.000	90.242	2.7	0.000	0.000	0.000	0.000	F-Bus 11	-1.043	-0.854	78.4	77.4
								F-Bus 13	0.788	0.639	59.0	77.7
								RB 11	0.254	0.215	19.4	76.5
F-Bus 13	11.000	90.236	2.7	0.000	0.000	0.000	0.000	F-Bus 12	-0.788	-0.639	59.0	77.7
								F-Bus 14	0.758	0.617	56.8	77.6
								RB 12	0.030	0.023	2.2	79.4
F-Bus 14	11.000	90.234	2.7	0.000	0.000	0.000	0.000	F-Bus 13	-0.758	-0.617	56.8	77.6
								F-Bus 15	0.371	0.308	28.0	76.9
								RB 13	0.387	0.308	28.8	78.2
F-Bus 15	11.000	90.232	2.7	0.000	0.000	0.000	0.000	F-Bus 14	-0.371	-0.308	28.0	76.9
								F-Bus 16	0.169	0.134	12.6	78.3
								RB 14	0.202	0.174	15.5	75.7
F-Bus 16	11.000	90.232	2.7	0.000	0.000	0.000	0.000	F-Bus 15	-0.169	-0.134	12.6	78.3
								F-Bus 17	0.165	0.131	12.2	78.3
								RB 15	0.004	0.003	0.3	80.0
F-Bus 17	11.000	90.231	2.7	0.000	0.000	0.000	0.000	F-Bus 16	-0.165	-0.131	12.2	78.3
								F-Bus 18	0.073	0.059	5.5	77.7
								RB 16	0.092	0.072	6.8	78.8
F-Bus 18	11.000	90.230	2.7	0.000	0.000	0.000	0.000	F-Bus 17	-0.073	-0.059	5.5	77.7
								RB 17	0.073	0.059	5.5	77.7
RB 1	0.440	97.529	-0.7	0.000	0.000	0.086	0.065	F-Bus 2	-0.086	-0.065	145.2	80.0
RB 2	0.440	55.626	-17.5	0.000	0.000	0.986	0.740	F-Bus 3	-0.986	-0.740	2908.0	80.0
RB 3	0.440	89.714	-0.7	0.000	0.000	0.123	0.092	F-Bus 4	-0.123	-0.092	224.4	80.0
RB 4	0.440	94.670	1.3	0.000	0.000	0.008	0.006	F-Bus 5	-0.008	-0.006	14.6	80.0
RB 5	0.440	75.207	-7.1	0.000	0.000	0.635	0.476	F-bus 6	-0.635	-0.476	1385.2	80.0
RB 6	0.440	89.057	0.3	0.000	0.000	0.298	0.223	F-Bus 7	-0.298	-0.223	548.5	80.0
RB 7	0.440	91.120	1.6	0.000	0.000	0.029	0.022	F-Bus 8	-0.029	-0.022	51.7	80.0
RB 8	0.440	85.244	-1.1	0.000	0.000	0.542	0.406	F-Bus 9	-0.542	-0.406	1042.3	80.0
RB 9	0.440	80.677	-2.6	0.000	0.000	0.775	0.581	F-Bus 10	-0.775	-0.581	1575.0	80.0
RB 10	0.440	86.928	1.2	0.000	0.000	0.077	0.058	F-Bus 11	-0.077	-0.058	144.9	80.0
RB 11	0.440	84.399	-0.6	0.000	0.000	0.249	0.187	F-Bus 12	-0.249	-0.187	483.9	80.0
RB 12	0.440	88.953	2.1	0.000	0.000	0.030	0.022	F-Bus 13	-0.030	-0.022	54.8	80.0
RB 13	0.440	85.966	0.2	0.000	0.000	0.000	0.000	C-Bus1	0.381	0.278	720.2	80.8

								F-Bus 14	-0.381	-0.278	720.2	80.8
RB 14	0.440	80.994	-1.2	0.000	0.000	0.191	0.143	F-Bus 15	-0.191	-0.143	387.3	80.0
RB 15	0.440	90.184	2.7	0.000	0.000	0.004	0.003	F-Bus 16	-0.004	-0.003	8.1	80.0
RB 16	0.440	88.221	1.6	0.000	0.000	0.091	0.068	F-Bus 17	-0.091	-0.068	169.2	80.0
RB 17	0.440	85.107	0.5	0.000	0.000	0.071	0.053	F-Bus 18	-0.071	-0.053	136.7	80.0

For more accuracy, the ETAP simulation has been simulated and generates the load flow analysis report of the input data. The given data is per day power consumption in KW after the load flow analysis feeder power factor is unbalanced with voltage drop. The voltage drop is between 8-10%, and the power factor drop is in between 20-30%. This issue has been rectified through load flow analysis by the Newton-Raphson Method in the ETAP simulation.

RESULT AND DISCUSSION

According to figures 1 (a) and (b), the overloading is occurring in the DT 2, 3, 5, 8, 9, 10, 11, 14 and 17. To resolve this overloading issue, modifications have been made in the DT ratings. Thus, the DT rating has been modified according to the load connected in the DTs and the value of DT has been modified, which is represented in Table 4. It represents an old rating of the DT with a new rating, along with the DT numbers. Simultaneously, Table 5 represents the new DT value, which has been added in the feeder to balance and manage the overloading. Due to these changes in voltage drop has been reduced gradually. These new DTs are DT 2.1, 2.2, 5.1, 8.1 and 9.1 ratings of the DTs were 750 kVA, 1000kVA, 500 kVA, 500 kVA and 500 kVA, respectively. Due to this rating modification voltage in DTs has been improved and the power losses have been reduced in the feeder.

Table 4. Distribution transformer rating modification

SI. No.	Distribution Transformer	Old Rating (KVA)	New Rating (KVA)
1	DT-2	250	600
2	DT-3	100	500
3	DT-5	250	500
4	DT-8	500	500
5	DT-9	500	500
6	DT-10	100	500
7	DT-11	250	500
8	DT-14	100	500
9	DT-17	63	250

Figure 2 depict the simulation diagram of load low analysis of modified radial system SLD with solar system and with solar and capacitor bank.

Table 5. New distribution transformer rating

SI. No.	Distribution Transformer	Rating (KVA)
1	DT-2.1	750
2	DT-2.2	1000
3	DT-5.1	500
4	DT-8.1	500
5	DT-9.1	500
6	DT-9.2	250

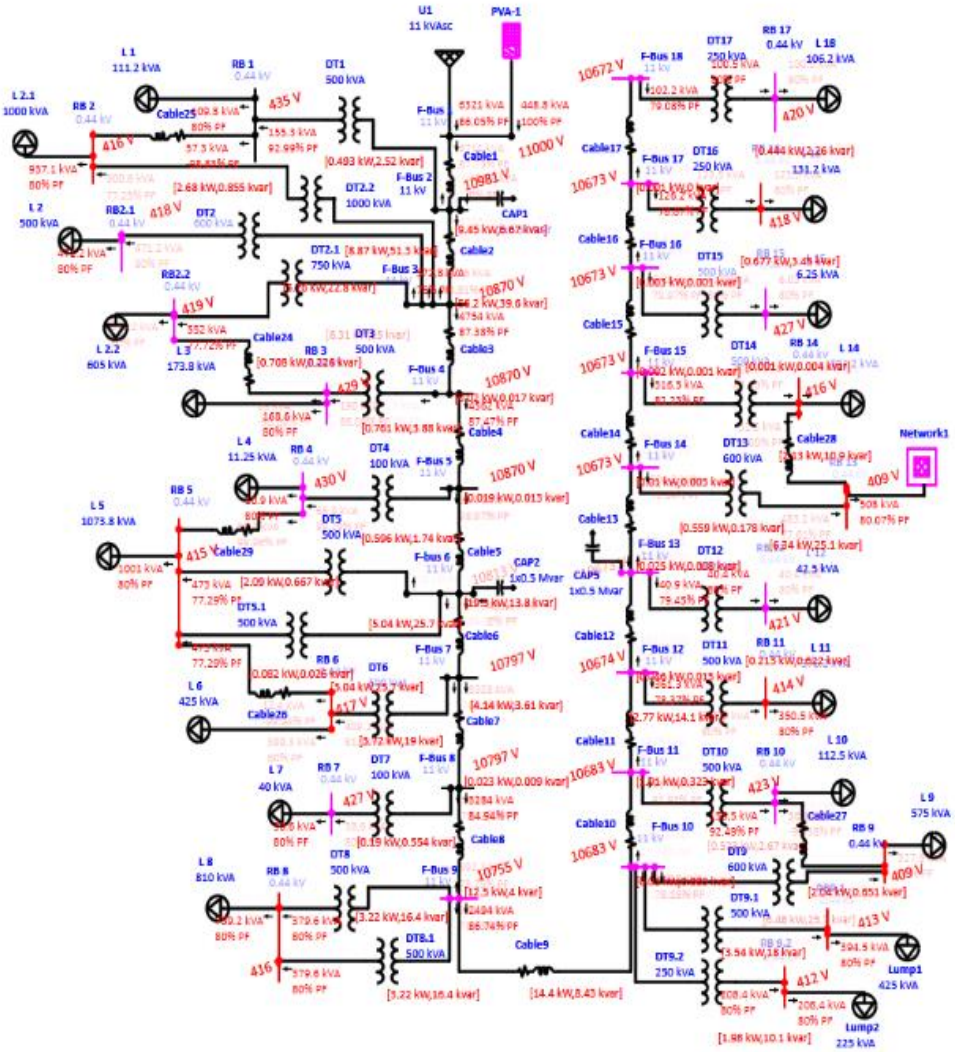

(a)

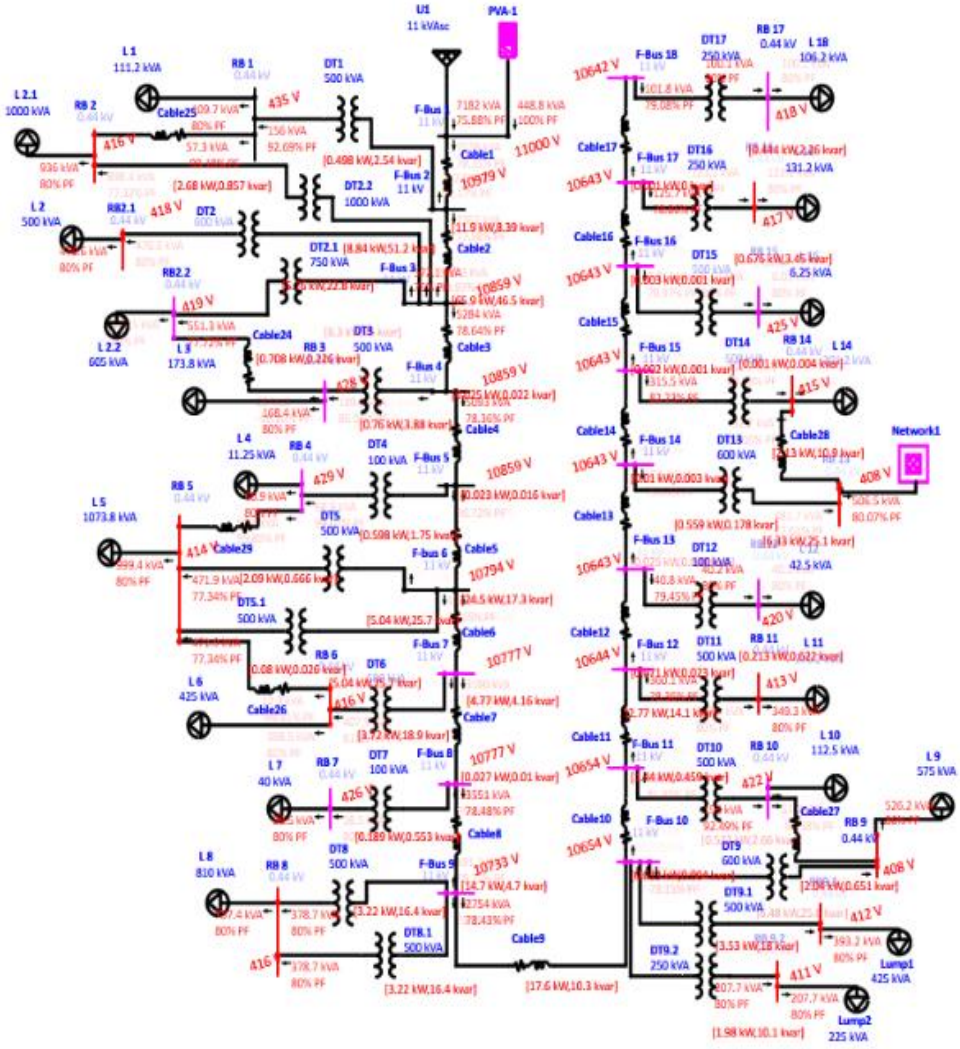

(b)

Figure 2. (a) Simulation diagram of Load low Analysis of Modified Radial System SLD with Solar System, (b) Simulation diagram of Load Flow Analysis of Modified Radial System SLD with Solar and capacitor bank

Figure 2 (a) represents the single-line diagram of the modified radial system with the solar. In this SLD, a solar panel has been added to the feeder grid supply to fulfil the power demand at peak hours for the consumers. The modified SLD with solar array represents the voltage improvement in the feeder. Thus, the voltage has been improved by the capacitor bank. Here, the capacitor is working as a power factor booster, which is represented in Figure 2 (b).

In this SLD, solar energy has been added to reduce the overloading from grid solar energy is supplying the energy to balance the radial flow of power in the feeder. Hence, through the simulation of modified radial system SLD with solar by the process of load flow analysis gives the result as voltage of the feeder gets balanced.

Table 6 represents the value of capacitor which is used in modified radial and cyclic system with a solar to improve the power factor. Which is shown in the figure 2 (b) and 3 (b). The representation of Cyclic system SLD with solar and solar with capacitor bank is another approach to utilize the maximum power from the grid with minimum loss. In this case, voltage improvement is occurring with the power factor improvement which is important for the stabilized power system in the feeder from the grid. It is represented in figure 3 (a) and 3 (b).

Table 6. Capacitor details of the feeder

Name	Rating	MVAR	Connected in Bus
CAP1	0.5*1 Mvar	0.5	F-Bus 2
CAP2	0.5*1 Mvar	0.5	F-Bus 6
CAP5	0.5*1 Mvar	0.5	F-Bus 13

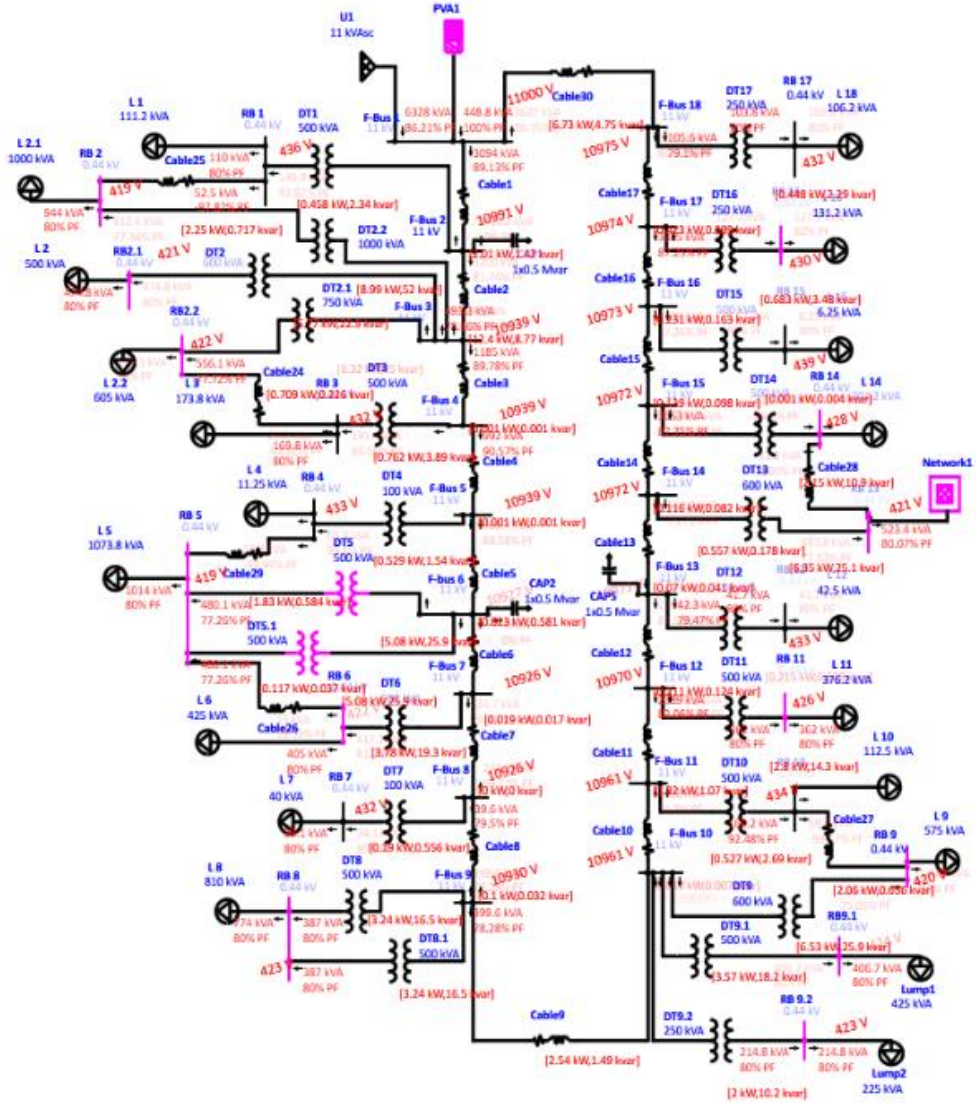

(a)

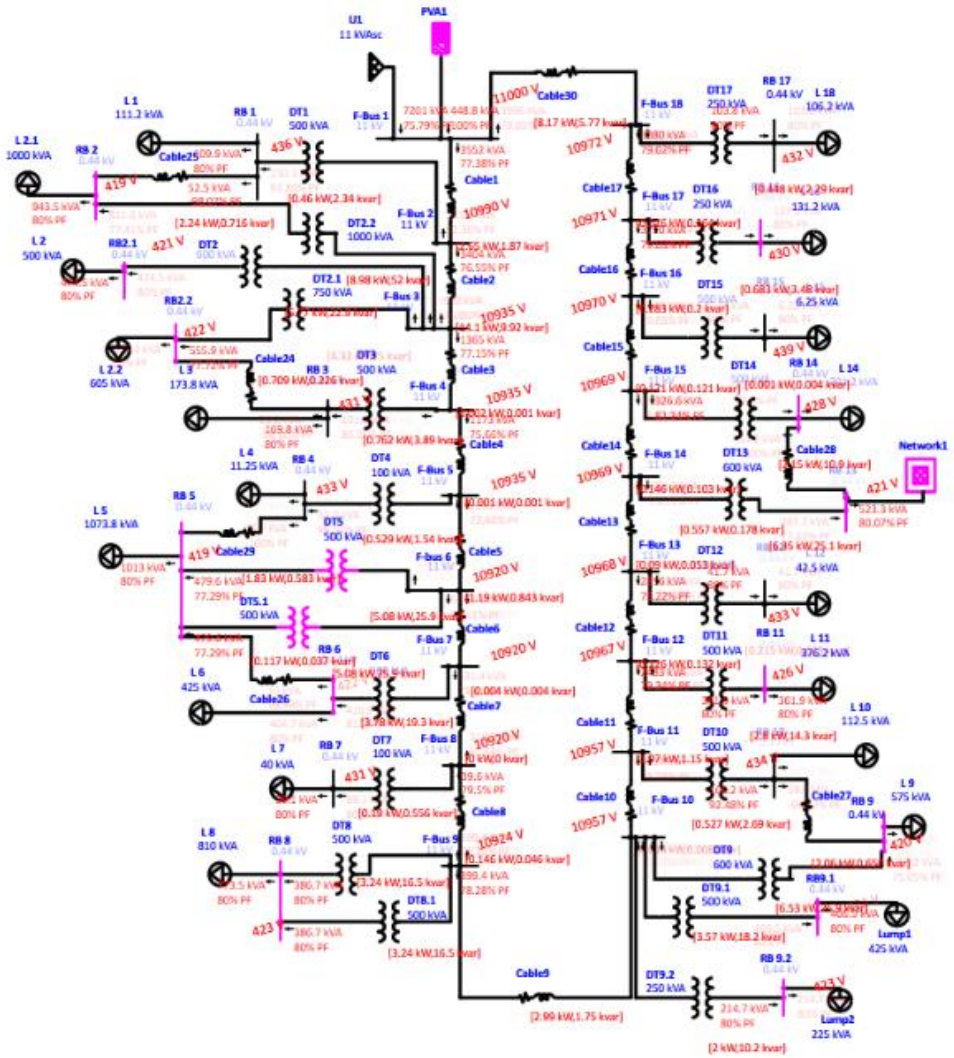

(b)

Figure 3. (a) Simulation diagram of Load Flow Analysis of Modified Cyclic System SLD with Solar System, (b) Simulation diagram of Load Flow Analysis of Modified Cyclic System SLD with Solar and capacitor bank

When the comparison comes to the role, it should have some standard value. The standard value of voltage is 11 kV and a power factor of 0.8 to 0.85 has to be maintained in the feeder and maintained for a healthy system for a smooth power flow process. As for the given condition, there are 5 stages of modification. Those are the Existing System, Modified Radial with Solar, Radial Solar with Capacitor Bank, Modified Cycle with Solar and Cyclic Solar with Capacitor Bank. These conditions were tested with the simulation through ETAP by the Newton-Raphson method for load flow analysis. It represents here the voltage improvement from an existing system to the other four compared systems. In the existing system, the maximum voltage drop occurs at 10-12% in the feeder. To improve this voltage or to reduce the voltage drop simulation has been conducted in 4 different stages. The existing system is the real unmodified data with all the real input data implemented in the SLD.

Figures 4 and 5 depict respectively the voltage comparison graph of feeder bus and residential bus.

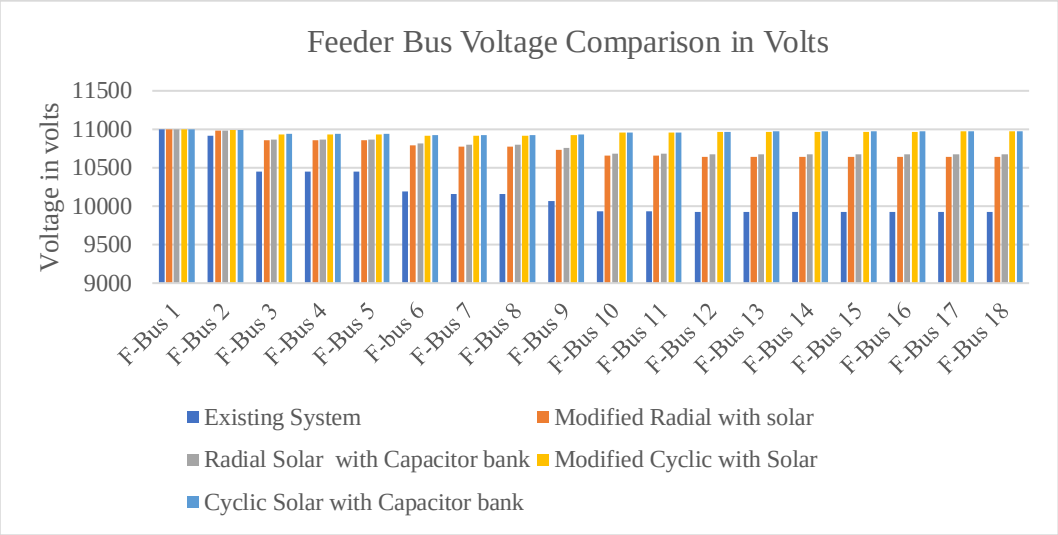

Figure 4. Voltage comparison graph of feeder Bus

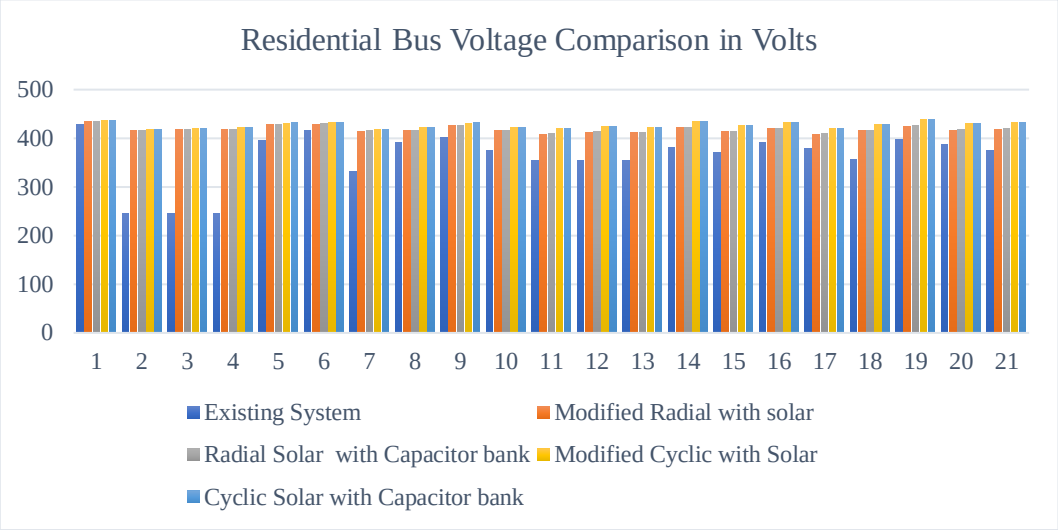

Figure 5. Voltage comparison graph of residential bus

The 2nd stage is modified radial with a solar system for power balancing and to improve the voltage. This will reduce the voltage drop problem in the feeder. The 3rd stage is radial solar with the capacitor bank system. It helps to boost the feeder voltage as well as the power factor. The 4th stage is cyclic solar with a capacitor bank system. It is a cycle system, which will improve the voltage of the feeder as well as the power factor. Thus, with the comparison of these all five stages. Each stage has an improvement in voltage, especially radial solar with capacitor bank and cyclic solar with capacitor bank in these two stages voltage improvement is maximum in the feeder. Due to this stage 98-99% of the voltage has been improved in the feeder. These stages have been implemented with

the feeder buses and residential buses. Hence, each system has to improve in voltage after applying these changes to the stages in the feeder, which are shown in figures 4 and 5.

Figures 6 and 7 depict respectively the power factor comparison graph of the feeder bus and residential bus.

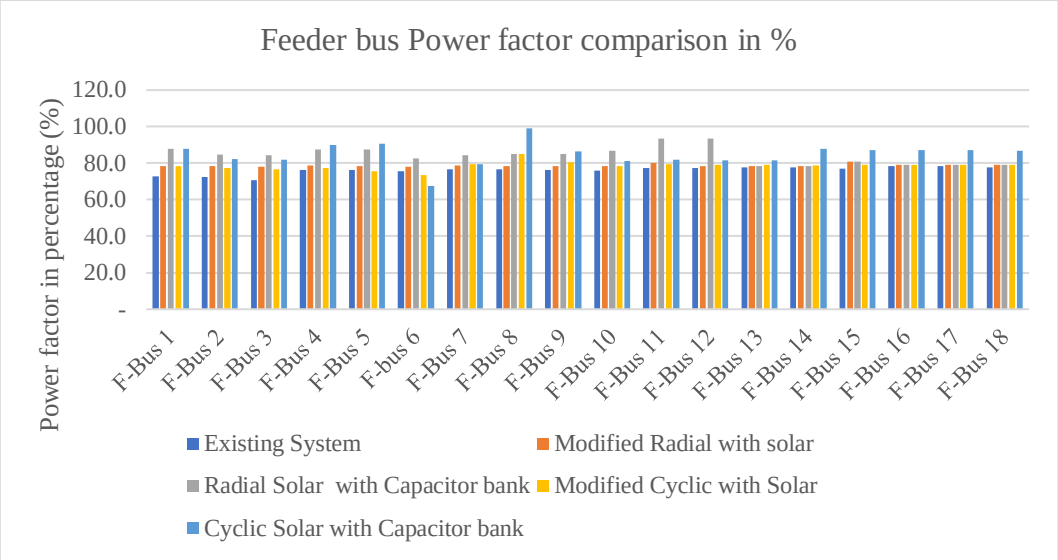

Figure 6. Power factor comparison graph of feeder bus

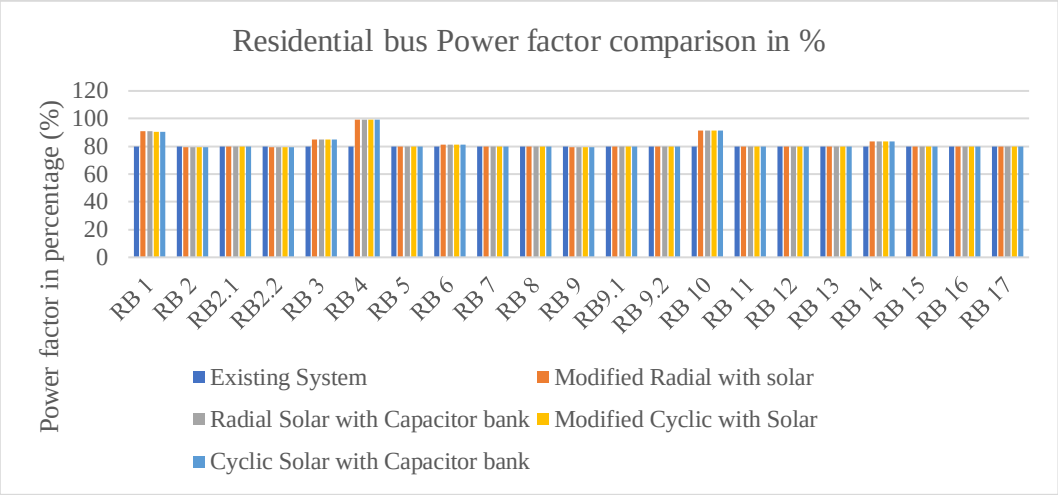

Figure 7. Power factor comparison graph of residential bus

The above graph represents the perfect comparison of the different stages of simulation done in ETAP through the load flow analysis by the Newton Raphson Method. There are 4 stages off representation of the power factor improvement. In the existing system, the real power factor of the feeder was 72-78%. In the 1st stage modified radial with the Solar System has improved 80-87% in the Power factor in the feeder. Which is better than the existing system power factor value. In the 2nd stage, radial solar with the capacitor bank system has improved 85-90% in the power factor of the feeder. which is better than the modified with solar system. The 3rd stage is radial solar with the capacitor bank system. It

helps to improve the bus power factor. Which will help to balance the voltage rating. The 4th stage is cyclic solar with a capacitor bank system. It is a cycle system, which will emphasize the power factor, and it will reduce the losses.

Due to this stage, 85-90% of the power factor has been improved in the feeder. These stages have been implemented with the feeder buses and residential buses for the power factor improvement. Hence, both the systems have improved the power factor after applying these changes in the stages of the feeder.

Figure 8 represents the overall power loss in the feeder in units and cost-wise. Five different systems have been simulated for the values for the simulation. In the process of simulation, the branch loss summary will represent the overall branch loss of the feeder. That branch loss value is only refreshed in Figure 8. In the existing system, total branch loss occurs 22437.6 units. According to the power cost of 1unit costs 6 rupees. So, the total cost loss is 134626 rupees. In modified radial with the solar system, the branch loss has been reduced to 5320.8 units and 31924.8 rupees. In a radial solar capacitor bank system, the branch loss has been reduced by modifying the radial with the solar system. Which reduced to 4754.4 units and 28526.4 rupees.

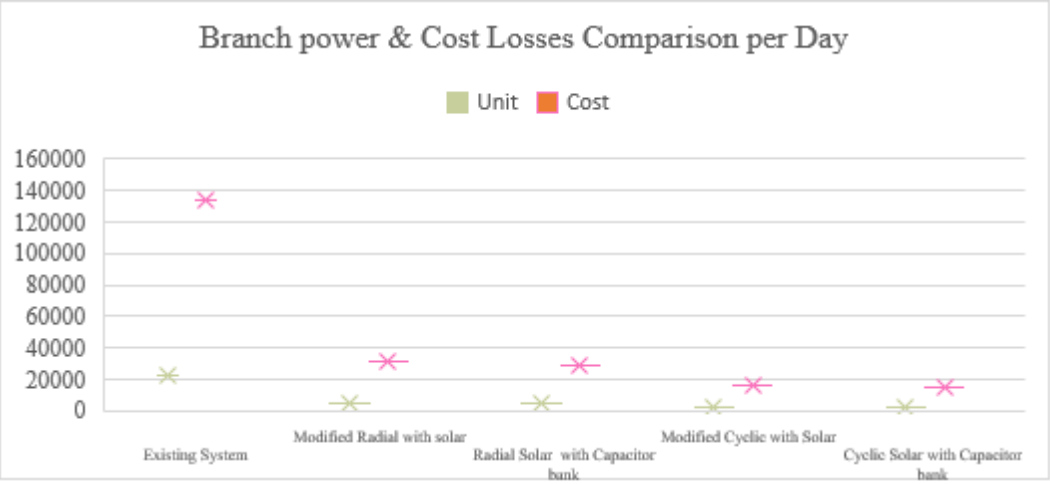

Figure 8. Power loss in units and cost loss comparison graph

In a modified cyclic with solar system, the branch loss has been reduced from radial solar with a capacitor bank system. It reduces to 2714.4 units and 16286.4 rupees. After that, finally, cyclic solar with a capacitor bank system has the least branch loss compared to all the other four systems. It is 2594.4 units and 15566.4 rupees for the system. This is represented in the graph of Figure 8.

Voltage Profile and Power Factor Enhancement:

The load flow results demonstrate the quantitative impact of the proposed systems on key network metrics, see Table 7. The introduction of the cyclic system significantly improves voltage profile and drastically cuts power losses (57.6% reduction) compared to the base radial configuration. Furthermore, the SAIFI metric clearly illustrates the

reliability benefit of the looped structure, moving from a standard radial vulnerability (2.5 interruptions/year) to a high-redundancy system (0.8 interruptions/year).

Table 7. Optimal results in different scenarios

Metric	Base Radial	Radial + PV/Capacitor	Proposed Cyclic + PV/Capacitor
Minimum Bus Voltage (p.u.)	0.893 p.u.	0.941 p.u.	0.964 p.u. (4.4% improvement over Radial + PV)
Total Real Power Loss (kW)	184.2 kW	102.5 kW	78.1 kW (57.6% reduction from Base)
Substation Power Factor	0.85 Lagging	0.95 Lagging	0.98 Lagging
Voltage Deviation Index (VDI)	0.0034	0.0011	0.00063 (81% reduction from Base)
System Average Interruption Frequency Index (SAIFI)	2.5 times/yr	2.5 times/yr	0.8 times/yr (Modeling the impact of cyclic redundancy)

Sensitivity Analysis: Impact of Solar Irradiance:

To establish the robustness of the proposed system, a sensitivity analysis has been performed by varying the solar irradiance (Global Horizontal Irradiance, GHI) used in the PV model by ±20% relative to the nominal design point (500 kW output), see Table 8. This simulates varying weather conditions, from clear sky (high irradiance) to moderate cloud cover (low irradiance).

Table 8. Sensitivity analysis (impact of solar irradiance)

Scenario	Irradiance Level	PV Output	Minimum Bus Voltage (p.u.)	Total Real Power Loss (kW)	VDI
Low Irradiance	-20% GHI	400 kW	0.950 p.u.	88.5 kW	0.00085
Nominal (Baseline)	100% GHI	500 kW	0.964 p.u.	78.1 kW	0.00063
High Irradiance	+20% GHI	600 kW	0.975 p.u.	69.3 kW	0.00050

The analysis confirms that even in the worst-case low-irradiance scenario (PV output dropping to 400 kW), the minimum bus voltage remains above the critical 0.95 p.u. threshold (at 0.950 p.u.). The VDI only increases by 35% compared to the optimal case, demonstrating that the combination of the cyclic structure and strategic capacitor placement successfully isolates the network from extreme voltage instability due to solar variability. This quantitative evidence validates the design's stability.

CONCLUSION

The integration of solar energy into radial and cyclic single-line diagram (SLD) systems has demonstrated significant improvements in voltage reliability and power factor enhancement. Through the implementation of adaptive demand-side management (DSM) techniques and load flow analysis using ETAP simulation, the study effectively addressed the challenges of voltage drops and power factor imbalances in the existing electrical distribution network.

The results indicate a substantial reduction in power losses across various configurations. Specifically, the existing system experienced a total branch loss of 22,437.6 units, translating to a cost loss of approximately 134,626 rupees. In contrast, the modified radial system with solar integration reduced branch losses to 5,320.8 units (a reduction of about 76.3%) and costs to 31,924.8 rupees. The addition of a capacitor bank further optimized the radial solar system, achieving branch losses of 4,754.4 units (a 78.8% reduction) and costs of 28,526.4 rupees.

The modified cyclic system with solar energy and capacitor banks yielded the most favourable results, with branch losses decreasing to 2,594.4 units, representing an impressive reduction of approximately 88.4% and a cost loss of 15,566.4 rupees. Overall, the study highlights the effectiveness of integrating renewable energy sources and advanced DSM strategies in enhancing the reliability and efficacy of power distribution systems, ultimately leading to significant operational cost savings and improved power quality.

Furthermore, the sensitivity analysis confirmed the system's stability, showing that even with a 20% reduction in solar power output, the voltage profile metrics (Minimum Voltage and VDI) remain well within acceptable operational limits, affirming the design's reliability against environmental uncertainty.

Additionally, this distribution management system can be implemented into the Demand-Side-Management of different types of feeders with multi-directional solutions. This presented reference model can be implemented in the commercial and industrial sectors for voltage improvement and power factor improvement under other circumstances.

AUTHOR CONTRIBUTIONS

Conceptualization: J.G.; Methodology: J.G., and G.S.; Formal analysis and investigation: J.G., and G.S.; Writing - original draft preparation: J.G.; Writing - review and editing: G.S.; Supervision: G.S.

CONFLICT OF INTEREST

The authors declare that they have no known competing financial interests or personal relationships that could have appeared to influence the work reported in this paper.

ACKNOWLEDGMENTS

The research outcomes of this manuscript were supported by the Department of Electrical and Electronics Engineering, Aarupadai Veedu Institute of Technology, Vinayaka Missions Research Foundation (DU), Chennai-603104, India, for their valuable guidance and technical support.

REFERENCES

1. Nebey, A.H. Recent Advancement in Demand Side Energy Management System for Optimal Energy Utilization. *Energy Reports* **2024**, *11*, 5422–5435.
2. Hamid, C., Aziz, D., Zamzoum, O., El Idrissi, A. Robust Control System for DFIG-Based WECS and Energy Storage in Reel Wind Conditions. *EAI Endorsed Transactions on Energy Web* **2024**, *11*, 1–6.
3. Hamid, C., Aziz, D., Zamzoum, O., El Idrissi, A., Zawbaa, H.M., Zeinoddini-Meymand, H., Kamel, S. Intelligent Control of the Power Generation System Using DSPACE. *Electronics Letters* **2024**, *60*(9), 1-4.
4. El Idrissi, A., Derouich, A., Mahfoud, S., El Ouanjli, N., Chojaa, H., Chantoufi, A. Bearing Faults Diagnosis by Current Envelope Analysis under Direct Torque Control Based on Neural Networks and Fuzzy Logic—A Comparative Study. *Electronics* **2024**, *13*(16), 3195.
5. Bakare, M. S., Abdulkarim, A., Zeeshan, M., Shuaibu, A.N. A Comprehensive Overview on Demand Side Energy Management towards Smart Grids: Challenges, Solutions, and Future Direction. *Energy Informatics* **2023**, *6*(1), 4.
6. Çakıl, F., Tekdemir, İ.G. A Novel Probabilistic Load Shifting Approach for Demand Side Management of Residential Users. *Energy and Buildings* **2024**, *323*, 114751.
7. Misra, S., Dey, B., Panigrahi, P.K.; Ghosh, S. A Swarm-Intelligent-Based Load-Shifting Strategy for Clean and Economic Microgrid Operation. *ISA Transactions* **2024**, *147*, 265–287.
8. El-Afifi, M.I., Sedhom, B.E., Eladl, A.A., Elgamal, M., Siano, P. Demand Side Management Strategy for Smart Building Using Multi-Objective Hybrid Optimization Technique. *Results in Engineering* **2024**, *22*, 102265.
9. Glazunova, A., Kovalchuk, D., Tomin, N, Iskakov, A. Design of Daily Load Profiles in Commercial and Industrial Microgrids Based on Renewable Energy Sources. *IFAC-PapersOnLine* **2024**, *58*(13), 272–277.
10. Bhullar, S., Ghosh, S. Optimal Integration of Multi Distributed Generation Sources in Radial Distribution Networks Using a Hybrid Algorithm. *Energies* **2018**, *11*(3), 628.
11. Askar, S., Sadikova, A., Mohammed, R.J., Khalaf, H.H., Ghazaly, N.M., Radhan, R.P., Candra, O. Optimal Demand Management of Smart Energy Hybrid System Based on Multi-Objective Optimization Problem. *Science and Technology for Energy Transition* **2024**, *79*, 53.
12. Anthony, M., Prasad, V., Kannadasan, R., Mekhilef, S., Alsharif, M.H., Kim, M.K., Jahid, A., Aly, A.A. Autonomous Fuzzy Controller Design for the Utilization of Hybrid PV–Wind Energy Resources in Demand Side Management Environment. *Electronics* **2021**, *10*(14), 1618.
13. Ayub, M.A., Khan, H., Peng, J., Liu, Y. Consumer-Driven Demand-Side Management Using K-Mean Clustering and Integer Programming in Standalone Renewable Grid. *Energies* **2022**, *15*, 1006.
14. García-Vilela, L. M., Huamán-Romaní, Y.L., Aragon-Navarrete, R.N., Zegarra, S.D., Carbajal, E.N. Energy Scheduling in the Multiple Energy System with Optimal Operation of the Responsive Loads. *International Journal of Integrated Engineering* **2024**, *16*(5), 341–358.

15. Kim, Y., Han, J., Yu, S. Establishment of Energy Management Strategy of 50 kW PEMFC Hybrid System. *Energy Reports* **2023**, *9*, 2745–2756.
16. Wu, J., Li, S., Fu, A., Cvetković, M., Palensky, P., Vasquez, J.C., Guerrero, J. M. Hierarchical Online Energy Management for Residential Microgrids with Hybrid Hydrogen–Electricity Storage System. *Applied Energy* **2024**, *363*, 123020.
17. Sharma, P., Saini, K.K., Mathur, H.D., Mishra, P. Improved Energy Management Strategy for Prosumer Buildings with Renewable Energy Sources and Battery Energy Storage Systems. *Journal of Modern Power Systems and Clean Energy* **2024**, *12*(2), 381–392.
18. Candra, O., Pradhan, R., Shukhratovna, A.N., Mohammed, B.A., Hamzah, A.K., Alzubaidi, L.H., Shoja, S.J. Optimal Day-Ahead Energy Scheduling of the Smart Distribution Electrical Grid Considering Hybrid Demand Management. *Smart Grids and Sustainable Energy* **2024**, *9*(2), 31.
19. Ahmad, S. Y., Hafeez, G., Aurangzeb, K., Rehman, K., Khan, T.A., Alhussein, M. A Sustainable Approach for Demand Side Management Considering Demand Response and Renewable Energy in Smart Grids. *Frontiers in Energy Research* **2023**, *11*, 1212304.
20. Alcani, M., Shuli, M., & Hoxha, A. Pumped-Storage Energy Systems for the Drin River Cascade: A Case Study. *Journal of Transactions in Systems Engineering*, **2025**, *3*(3), 508–521.
21. Acharya, S. K., Yu, H., Wi, Y.M., Lee, J. Multihousehold Load Forecasting Based on a Convolutional Neural Network Using Moment Information and Data Augmentation. *Energies* **2024**, *17*(4), 902.
22. Bardhi, A., Eski, A., Leka, B., Dhoska, K. The Impact of Solar Power Plants on the Electricity Grid: A Case Study of Albania. *Eng* **2025**, *6*, 35.
23. Pal, D., Kumar, S., Tudu, B., Mandal, K.K., Chakraborty, N. Efficient and Automatic Reconfiguration and Service Restoration in Radial Distribution System Using Differential Evolution. In *Proceedings of the International Conference on Frontiers of Intelligent Computing: Theory and Applications (FICTA)*; Springer: **2012**, pp. 365–372.
24. Kumar, S., Pal, D., Mandal, K.K., Chakraborty, N. Performance Study of a New Modified Differential Evolution Technique Applied for Optimal Placement and Sizing of Distributed Generation. In *Proceedings of the 4th International Conference on Swarm, Evolutionary, and Memetic Computing*; **2013**, pp. 189–198.
25. Kumar, S., Mandal, K.K., Chakraborty, N. Optimal Placement of Different Types of DG Units Considering Various Load Models Using Novel Multiobjective Quasi-Oppositional Grey Wolf Optimizer. *Soft Computing* **2021**, *25*(6), 4845–4864.
26. Ahmad, S., Afzal M.J., and Kazmi, S.A.A. Comparative Analysis of Radial and Looped Distribution Network Against Voltage Stability and Loadability with Distributed Generation. *5th International Symposium on Environment-Friendly Energies and Applications (EFEA)*, Rome, Italy, **2018**, pp. 1-6.
27. Ahmad, S., Asar, A.u. Reliability Enhancement of Electric Distribution Network Using Optimal Placement of Distributed Generation. *Sustainability* **2021**, *13*, 11407.
28. Wang, H., Chen, Q., Zhang, L., Yin, X., Zhang, Z., Wei, H., Chen, X. Research and Engineering Practice of Var-Voltage Control in Primary and Distribution Networks Considering the Reactive Power Regulation Capability of Distributed PV Systems. *Energies* **2025**, *18*, 2135.
29. Ellithy, K., et al. Optimal Shunt Capacitors Allocation in Distribution Networks Using Genetic Algorithm- Practical Case Study. *International Journal of Innovations in Energy Systems and Power* **2008**, *3*(1), 13-45.
30. Grisales-Noreña, L.F., Sanin-Villa, D., Montoya, O.D., Bolaños, R.I., Bonilla Rojas, K.X. Cost-Optimal Coordination of PV Generation and D-STATCOM Control in Active Distribution Networks. *Sci* **2026**, *8*, 8.
31. Chedid, R., Sawwas, A. Optimal placement and sizing of photovoltaics and battery storage in distribution networks. *Energy Storage* **2019**, *1*(4), e46.

32. Sa'ed, J.A., Wari, Z., Abughazaleh, F., Dawud, J., Favuzza, S., Zizzo, G. Effect of Demand Side Management on the Operation of PV-Integrated Distribution Systems. *Appl. Sci.* **2020**, *10*, 7551.
33. Pardhi, C., Khare, K., Choubey, A. Impact of Irradiance and Temperature on Electrical Parameters of Polycrystalline Photovoltaic Module: A Five Parameter Analysis. *International Journal of Recent Technology and Engineering* **2024**, *13*(2), 12–20.
34. Taufik, et al. Modeling and Load Flow Analysis of a Microgrid Laboratory. *IJSGSET Transactions on Smart Grid and Sustainable Energy* **2019**, *3*(2), 103-111.
35. Almasoudi, A.O., Habibullah, I.O. A Review on Load Flow Analysis Modern Techniques, *International Journal of Engineering Research & Technology*, **2021**, *10*(12), 108-111.
36. Fuchs, A., Lohmann, A., & Gebremedhin, A. Transitioning Towards a Sustainable Energy System: A Case Study of Baden-Württemberg. *International Journal of Innovative Technology and Interdisciplinary Sciences*, **2024**, *7*(4), 157–197.
37. Amoako Kyeremeh, K., Kofi Otchere, I., Twum Duah, N., & Owusu, J. Distribution Network Reconfiguration Considering Feeder Length as a Reliability Index. *International Journal of Innovative Technology and Interdisciplinary Sciences*, **2023**, *6*(1), 1100–1111.
38. Bai, W., Zhang, Z., Zhang, Y., Zhao, W., Zhang, B. Virtual Coupling Control of Photovoltaic–Energy Storage Power Generation System for Efficient Power Support. *Energy Reports* **2024**, *12*, 1742–1752.